Title

Numerical Integration Scheme Using Singular Perturbation Method

ISBN

978-0-7918-5596-6

Authors

Gil, Gibin
Sanfelice, Ricardo G
Nikravesh, Parviz E

Publication Date

2013-08-04

DOI

10.1115/detc2013-13330

Peer reviewed

Proceedings of the ASME 2013 International Design Engineering Technical Conferences & Computers and Information in Engineering Conference
IDETC/CIE 2013
August 4-7, 2013, Portland, Oregon, USA

DETC2013-13330

NUMERICAL INTEGRATION SCHEME USING SINGULAR PERTURBATION METHOD

Gibin Gil
Ricardo G. Sanfelice
Parviz E. Nikravesh
Department of Aerospace and Mechanical Engineering
University of Arizona
Tucson, Arizona 85721-0119
Email: {gil, sricardo, pen}@email.arizona.edu

ABSTRACT

Some multi degree-of-freedom dynamical systems exhibit a response that contain fast and slow variables. An example of such systems is a multibody system with rigid and deformable bodies. Standard numerical integration of the resultant equations of motion must adjust the time step according to the frequency of the fastest variable. As a result, the computation time is sacrificed. The singular perturbation method is an analysis technique to deal with the interaction of slow and fast variables. In this study, a numerical integration scheme using the singular perturbation method is discussed, its absolute stability condition is derived, and its order of accuracy is investigated.

INTRODUCTION

Quite often, the solution of a state equation has some variables evolving in time faster than other variables, leading to the classification of variables as slow and fast. Such systems are called highly oscillatory system and the computation of their solutions is referred to as a multiple-timescale problem [1].

Standard numerical methods require a short step size to capture the dynamics of the fast variables. The computational cost of solving the entire system is dictated by the time scale of the fast variables and, hence, the numerical efficiency can become an important issue.

Multirate methods were proposed to improve the numerical efficiency when solving highly oscillatory dynamical systems. The methods exploit the different time scales by using different step sizes for the subsystems. This kind of approach was applied for electric circuit simulation [2], molecular dynamics simulation [3, 4], and stellar problems [5]. There have been many attempts to apply multirate method to mechanical systems, especially multibody systems. In [6], partitioned Runge-Kutta method was employed to simulate the dynamics of vehicle systems that contain subsystems with high frequency response characteristics. The multirate method based on the Backward Differentiation Formula (BDF) was proposed and applied for the simulation of the aero-elastic model of helicopter [7]. In [8], the simulation of pantograph and catenary was conducted with a multirate method.

In this study, a numerical integration method that utilizes the local linearization method [9, 10] and the singular perturbation method [11] to deal with the coupling between the fast and slow variables is introduced. The singular perturbation method is an analysis technique to deal with the interaction of slow and fast variables. The proposed numerical integration method can capture the fast dynamics using the local linearization method while the dynamics of the slow variable is computed by a conventional numerical method with the help of the invariant manifold of singular perturbation theory. The local linearization method is an exponential method which is based on the piecewise linear approximation of the state equation through a first-order Taylor expansion at each time step. The solution at the next time step is determined by the analytic solution of the approximated linear system. This paper discusses the absolute

stability condition and accuracy of the proposed numerical integration method and demonstrates its advantage by numerical experiments.

SINGULAR PERTURBATION

The singular perturbation model associated with a dynamical system is a state model where the derivatives of some of the states are multiplied by a small positive parameter ε [1]:

$$\dot{x} = f(t,x,z,\varepsilon) \tag{1a}$$
$$\varepsilon\dot{z} = g(t,x,z,\varepsilon) \tag{1b}$$

It is assumed that the functions f and g are continuously differentiable and $x \in \mathbb{R}^n, z \in \mathbb{R}^m$. By setting $\varepsilon = 0$, Eqn. (1b) becomes

$$0 = g(t,x,z,0) \tag{2}$$

If Eqn. (2) has $k \geq 1$ isolated real roots

$$z = h_i(t,x), \quad i = 1,2,\ldots,k \tag{3}$$

then Eqns. (1a)-(1b) are in standard form and they reduce to

$$\dot{x} = f(t,x,h(t,x),0) \tag{4}$$

This model is called the *slow*, *reduced*, or *quasi-steady-state model*. With the new time variable $\tau = (t-t_0)/\varepsilon$, the so-called boundary-layer model is defined as

$$\frac{dy}{d\tau} = g(t,x,y+h(t,x),0), \quad \text{where } y = z - h(t,x) \tag{5}$$

A geometric view of the singular perturbed system and the reduced model can be obtained by the concept of invariant manifolds. For simplicity, we consider the autonomous singularly perturbed system

$$\dot{x} = f(x,z) \tag{6a}$$
$$\varepsilon\dot{z} = g(x,z) \tag{6b}$$

Let $z = h(x)$ be an isolated root of $0 = g(x,z)$. Then, the equation $z = h(x)$ is an invariant manifold for the system

$$\dot{x} = f(x,z) \tag{7a}$$
$$0 = g(x,z) \tag{7b}$$

When $\varepsilon = 0$, any trajectory starting in the manifold $z = h(x)$ will remain in that manifold for all positive time. The dynamics in this manifold can be described by the reduced model as

$$\dot{x} = f(x,h(x)) \tag{8}$$

Extending this concept to the case of nonzero ε, the invariant manifold for $\varepsilon > 0$ can be found in the following form:

$$z = H(x,\varepsilon) = H_0(x) + \varepsilon H_1(x) + \varepsilon^2 H_2(x) + \cdots \tag{9}$$

By differentiating $z = H(x,\varepsilon)$ with respect to t, we obtain

$$\frac{1}{\varepsilon} g(x,z) = \frac{\partial H}{\partial x}\dot{x} \tag{10}$$

and, after some rearrangement we obtain

$$0 = g(x,H(x,\varepsilon)) - \varepsilon \frac{\partial H}{\partial x} f(x,H(x,\varepsilon)) \tag{11}$$

which is called the manifold condition. The function $H(x,\varepsilon)$ must satisfy the manifold condition for all x in the region of interest. The invariant manifold $z = H(x,\varepsilon)$ is called a slow manifold for Eqns. (6a)-(6b). By setting $\varepsilon = 0$, it can be seen that

$$H_0(x) = h(x) \tag{12}$$

The first order term $H_1(x)$ can be determined from the manifold condition as follows. The manifold condition is

$$g(x,H(x,\varepsilon)) = \varepsilon \frac{\partial H}{\partial x} f(x,H(x,\varepsilon)) \tag{13}$$

We can obtain the following expression through series expansion of ε:

$$\begin{aligned} &g(x,h(x)) + \varepsilon \frac{\partial g}{\partial z}(x,h(x))H_1(x) + O(\varepsilon^2) \\ &= \varepsilon \frac{\partial h}{\partial x} f(x,h(x)) + O(\varepsilon^2) \end{aligned} \tag{14}$$

Since $g(x,h(x)) = 0$, $H_1(x)$ can be obtained as

$$H_1(x) = \left(\frac{\partial g}{\partial z}(x,h(x))\right)^{-1} \left(\frac{\partial h}{\partial x} f(x,h(x))\right) + O(\varepsilon^2) \tag{15}$$

if the Jacobian $[\partial g/\partial z]$ is nonsingular.

The invariant manifolds can be used for the design of control systems, where the reduced system is considered instead of the complicated full system. In [12], the control problem of multibody systems with rigid links and flexible joints was considered. It was shown that any control law that stabilizes the rigid system would stabilize the dynamics of the flexible system on the invariant manifold. The stability analysis is based on Lyapunov functions for the reduced system and the boundary-layer system as described in [1, 13]. Similar results were shown for hybrid control systems. In [14], it was shown that hybrid control can be achieved based on a simple plant model that ignores stable, fast actuator dynamics.

Another application of the singular perturbation theory is the computational singular perturbation (CSP) method that is widely used in combustion modelling and chemical kinetics analysis [15–17]. The CSP is essentially an algorithm to find the reduced system and match the initial conditions to the dynamics on the invariant manifolds. The CSP aims for reducing the dimension of the problem and obtaining the approximated long-term dynamics of the system more efficiently.

There have been attempts to obtain numerical solutions of stiff differential equations using the singular perturbation theory. Some equivalence can be found between stiff and singularly perturbed differential equations [18]. If x,z are assumed to be scalar and Eqns.(1a)-(1b) are linearized along its trajectory, they may be expressed as

$$\begin{Bmatrix} \dot{x} \\ \dot{z} \end{Bmatrix} = \begin{bmatrix} f_x & f_z \\ g_x/\varepsilon & g_z/\varepsilon \end{bmatrix} \begin{Bmatrix} x \\ z \end{Bmatrix}, \quad x,z \in \mathbb{R} \tag{16}$$

Examination of the Jacobian eigenvalues indicates that they spread more as the ε becomes smaller. One eigenvalue approaches zero while the other grows large in absolute value. Thus Eqn. (16) can be regarded as the linearized representation of a stiff system with widely separated eigenvalues. Here, x corresponds to slow variable and z corresponds to fast variable. In [19], the singular perturbation method was applied for the numerical method to solve stiff differential equations. Unlike conventional numerical methods, it performs better as the stiffness of the system increases. And this approach was extended to the ε-Independent Method [20], where the small parameter ε does not need to be identified. But in these methods, the transient part of the solution is neglected with the assumption that they decay exponentially. So, they can not be used for the highly oscillatory systems that contain eigenvalues of large imaginary part. The transient behavior of the system can not be obtained accurately even though the asymptotic behavior of the system can be reconstructed well.

NUMERICAL INTEGRATION SCHEME

In this section, a new numerical integration scheme for the multiple-timescale problems is discussed. The scheme is based on the concept of slow manifold in singular perturbation theory without requiring to identify the small perameter ε. The scheme is applicable to both stiffly decaying and highly oscillatory systems. It should be noted that the method in [19, 20] can be used only on stiffly decaying problems, which neglects the transient part of the solution.

Let us consider a system of ordinary differential equation as:

$$\dot{x} = f(x,z), \quad x(0) = \xi \tag{17a}$$
$$\dot{z} = g(x,z), \quad z(0) = \eta \tag{17b}$$

The state variable x corresponds to the slow part of the system and the variable z represents the fast part. We take the linear approximation for $g(x,z)$ as

$$\dot{z} = g(x,z) \approx g_x \cdot (x-\xi) + g_z \cdot (z-\eta) + g(\xi,\eta) \tag{18}$$

where

$$g_x = \frac{\partial g}{\partial x}\Big|_{(\xi,\eta)}, \; g_z = \frac{\partial g}{\partial z}\Big|_{(\xi,\eta)}$$

Now, z is decomposed into $\bar{z}$ and y, where $\bar{z}$ is the quasi-steady-state part of z:

$$z = \bar{z} + y \tag{19}$$

Furthermore, $\bar{z}$ is assumed to satisfy the following condition:

$$0 = g(x,\bar{z}) \tag{20}$$

If we take the approximation of Eqn. (18), the condition for $\bar{z}$ becomes

$$0 = g_x \cdot (x-\xi) + g_z \cdot (\bar{z}-\eta) + g(\xi,\eta) \tag{21}$$

and we obtain

$$\bar{z} = \eta - (g_z)^{-1} \left[g_x \cdot (x-\xi) + g(\xi,\eta) \right] := H(x) \tag{22}$$

Here, it is assumed that g_z is not singular. By plugging Eqn. (19) into Eqn. (18), the following equation is obtained:

$$\dot{\bar{z}} + \dot{y} = g_z \cdot y \tag{23}$$

It follows that

$$\begin{aligned}\dot{y} &= g_z \cdot y - \dot{\bar{z}} \\ &= g_z \cdot y - \frac{\partial H}{\partial x}\dot{x} \\ &\approx g_z \cdot y + (g_z)^{-1} g_x f(\xi,\eta)\end{aligned} \tag{24}$$

The initial condition for y can be determined as follows. Since

$$z(0) = \bar{z}(0) + y(0) \tag{25}$$

and

$$\bar{z}(0) = H(\xi) = \eta - (g_z)^{-1} g(\xi,\eta) \tag{26}$$

we have

$$y(0) = \eta - \bar{z}(0) = (g_z)^{-1} g(\xi,\eta) \tag{27}$$

The dynamics of x can be approximated as:

$$\dot{x} = f(x,z) = f(x,\bar{z}+y) \approx f(x,H(x)) + f_z \cdot y(t) \tag{28}$$

Then, the numerical solution for x is obtained without the last term, $f_z \cdot y(t)$, and it is denoted by $\hat{x}$. Any conventional numerical method can be used since the equation

$$\dot{x} = f\left(x, H(x)\right), \quad x(0) = \xi \tag{29}$$

depends on x and has slow dynamics. The complete numerical solution for x is obtained by adding the effect of $f_z \cdot y(t)$ as:

$$x(h) = \hat{x} + \int_0^h f_z \cdot y(\tau) d\tau \tag{30}$$

The superposition in Eqn. (30) is possible because the effect of $f_z \cdot y(t)$ on x is small. The variable x having slow dynamics implies that the effect of f_z is not dominant and the main contribution of z on x is taken into consideration by $H(x)$. The last term on the right hand side of Eqn. (30) involves the integration of y. The dynamics of y is approximated as linear differential equation

$$\dot{y} = g_z \cdot y + \gamma, \quad \gamma := (g_z)^{-1} g_x f(\xi,\eta) \tag{31}$$

The analytic solution for y is given as

$$y(t) = e^{g_z t}\sigma + \int_0^t e^{g_z(t-s)}\gamma ds, \quad \sigma = (g_z)^{-1} g(\xi,\eta) \tag{32}$$

Therefore, the last term of Eqn. (30) can be computed as

$$\begin{aligned}\int_0^h f_z \cdot y(\tau) d\tau &= f_z \int_0^h y(\tau) d\tau \\ &= f_z\Big(\int_0^h e^{g_z\tau}\sigma d\tau + \int_0^h \int_0^s e^{g_z(s-r)}\gamma dr ds\Big) \\ &= f_z\Big(g_z^{-1}(e^{g_z h} - I)\sigma + \int_0^h \int_0^s e^{g_z(s-r)}\gamma dr ds\Big)\end{aligned} \tag{33}$$

This integration can be performed using the exponential of the block matrix D which is defined as [21]:

$$\mathbf{D} = \begin{bmatrix} 0 & I & 0 \\ 0 & g_z & \gamma \\ 0 & 0 & 0 \end{bmatrix} \tag{34}$$

$$e^{\mathbf{D}t} = \begin{bmatrix} F_1(t) & G_1(t) & J_1(t) \\ 0 & F_2(t) & G_2(t) \\ 0 & 0 & F_3(t) \end{bmatrix} \tag{35}$$

where

$$\begin{aligned} F_1(t) &= I \\ F_2(t) &= e^{g_z t} \\ F_3(t) &= 1 \\ G_1(t) &= tI \\ G_2(t) &= \int_0^t e^{g_z(t-s)}\gamma ds \\ J_1(t) &= \int_0^t \int_0^s e^{g_z(s-r)}\gamma dr ds \end{aligned} \tag{36}$$

Thus, the solution for x can be obtained as

$$x(h) = \hat{x} + f_z\left(g_z^{-1}\left(F_2(h) - I\right)\sigma + J_1(h)\right) \tag{37}$$

Using the solution for x in Eqn. (37), the dynamics of y can be

approximated more accurately as

$$\begin{aligned}\dot{y} &= g_z \cdot y - \dot{\tilde{z}} \\ &= g_z \cdot y - \frac{\partial H}{\partial x}\dot{x} \\ &\approx g_z \cdot y + (g_z)^{-1} g_x \left(f(x,H(x)) + f_z \cdot y\right) \\ &\approx \left(g_z + (g_z)^{-1} g_x f_z\right) y + (g_z)^{-1} g_x f(x,H(x))\end{aligned} \tag{38}$$

We take a linear interpolation for $f(x,H(x))$ and treat it as a function of time for $t \in [0,h]$:

$$f(x,H(x)) \approx \left(1-\frac{t}{h}\right) f(x(0),H(x(0))) + \frac{t}{h} f(x(h),H(x(h))) \tag{39}$$

Then, the differential equation of y takes the form of nonautonomous linear equation as

$$\dot{y} = Ay + u(t) \qquad \forall\, t \in [0,h] \tag{40}$$

where

$$A = g_z + (g_z)^{-1} g_x f_z$$
$$u(t) = (g_z)^{-1} g_x \left(\left(1-\frac{t}{h}\right) f(x(0),H(x(0))) + \frac{t}{h} f(x(h),H(x(h)))\right)$$

and the solution for y can be obtained as

$$y(t) = e^{At} y(0) + \int_0^t e^{A(t-\tau)} u(\tau) d\tau \tag{41}$$

The computation for y can be achieved through the exponential of block matrix as discussed in [10]. Finally, the solution for z is determined by

$$z(h) = H(x(h)) + y(h) \tag{42}$$

This process can be generalized and a numerical solution can be obtained by for each time step. The numerical integration procedure can be summarized as:

1. Compute $\int_{t_n}^{t_{n+1}} y(\tau) d\tau$

$$\int_{t_n}^{t_{n+1}} y(\tau) d\tau = (g_z)^{-1} (F_2 - I)\, \sigma + J_1 \tag{43}$$

where

$$\begin{aligned}\gamma &= (g_z)^{-1} g_x f(x_n, z_n) \\ \sigma &= (g_z)^{-1} g(x_n, z_n) \\ F_2 &= e^{g_z h_n} \\ J_1 &= \int_0^{h_n} \int_0^s e^{g_z (s-r)} \gamma\, dr ds\end{aligned}$$

F_2 and J_1 are obtained from the exponential of block matrix $\mathbf{D}$ of Eqn. (34):

$$e^{\mathbf{D} h_n} = \begin{bmatrix} F_1 & G_1 & J_1 \\ 0 & F_2 & G_2 \\ 0 & 0 & F_3 \end{bmatrix} \tag{44}$$

2. Compute x_{n+1}
Here, the fourth-order Runge-Kutta method is used to compute $\hat{x}$:

$$x_{n+1} = \hat{x} + f_z \int_{t_n}^{t_{n+1}} y(\tau) d\tau \tag{45}$$

where

$$\begin{aligned}H(x) &= y_n - (g_y)^{-1} \left(g_x \cdot (x - x_n) + g(x_n, y_n)\right) \\ X_1 &= x_n \\ X_2 &= x_n + \frac{h_n}{2} f(X_1, H(X_1)) \\ X_3 &= x_n + \frac{h_n}{2} f(X_2, H(X_2)) \\ X_4 &= x_n + h_n f(X_3, H(X_3)) \\ \hat{x} &= x_n + \frac{h_n}{6} (f(X_1, H(X_1)) + 2f(X_2, H(X_2)) \\ &\quad + 2f(X_3, H(X_3)) + f(X_4, H(X_4)))\end{aligned}$$

3. Compute z_{n+1}

$$z_{n+1} = H(x_{n+1}) + y_{n+1} = H(x_{n+1}) + \sigma + \phi \tag{46}$$

ϕ is obtained from $e^{h_n \bar{\mathbf{D}}}$ by Theorem 1 in [21] as:

$$e^{h_n \bar{\mathbf{D}}} = \begin{bmatrix} e^{h_n A} & \int_0^{h_n} e^{A(t-s)} ds & \phi \\ 0 & 1 & h_n \\ 0 & 0 & 1 \end{bmatrix} \tag{47}$$

where

$$\bar{\mathbf{D}} = \begin{bmatrix} A & B & C \\ 0 & 0 & 1 \\ 0 & 0 & 0 \end{bmatrix}$$
$$A = g_z + (g_z)^{-1} g_x f_z$$
$$B = A\sigma + (g_z)^{-1} g_x f(x_n, H(x_n))$$
$$C = \frac{(g_z)^{-1} g_x}{h_n} \left(f(x_{n+1}, H(x_{n+1})) - f(x_n, H(x_n)) \right)$$

ABSOLUTE STABILITY ANALYSIS

For a given numerical method, the *region of absolute stability* is the region of the complex ξ-plane such that applying the method for the test equation $\dot{y} = \lambda y$, with $\xi = h\lambda$ from within this region, yields an approximate solution satisfying the absolute stability requirement, $|y_{n+1}| \leq |y_n|$ [22].

Generally, all Runge-Kutta methods can be written in the following form when applied to the test equation $\dot{y} = \lambda y$:

$$y_{n+1} = R(h\lambda)\, y_n \tag{48}$$

where R is called the stability function of the Runge-Kutta method. For the fourth-order Runge-Kutta method, the stability function is given as

$$R(\xi) = 1 + \xi + \frac{1}{2}\xi^2 + \frac{1}{6}\xi^3 + \frac{1}{24}\xi^4 \tag{49}$$

The region of absolute stability is the region where $|R(\xi)| \leq 1$ is satisfied. The absolute stability region of the fourth-order Runge-Kutta method (RK4) is shown in Fig. 1. Due to the symmetricity with respect to the x-axis, only the upper half of the stability region will be exhibited in the upcoming figures.

We consider the following test equation to analyze the absolute stability of the hybrid integration scheme. The same test equation was used in [7] to derive the absolute stability region of a multirate integration method based on BDF:

$$\begin{Bmatrix} \dot{x} \\ \dot{z} \end{Bmatrix} = \begin{bmatrix} \lambda_s & \mu \\ \delta & \lambda_f \end{bmatrix} \begin{Bmatrix} x \\ z \end{Bmatrix} \tag{50}$$

The parameters α and β are defined as follows. The parameter α indicates the ratio of the frequencies of the fast and slow variables. The parameter β indicates the strength of coupling between the fast and the slow variables. Introducing these parameters enables us to identify the absolute stability region in

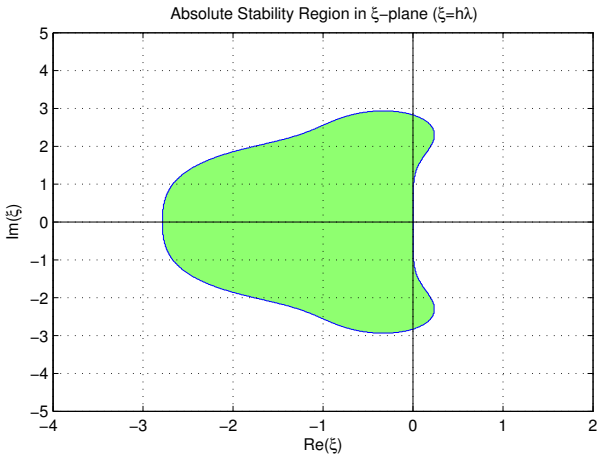

FIGURE 1. THE ABSOLUTE STABILITY REGION OF THE FOURTH-ORDER RUNGE-KUTTA METHOD

the ξ-plane:

$$\alpha = \frac{\lambda_f}{\lambda_s}, \quad \beta = \frac{\delta}{\lambda_f} = \frac{\mu}{\lambda_s}, \quad \xi = h\lambda_s \tag{51}$$

The proposed numerical scheme is applied to the test equation and the condition for the absolute stability is derived. By applying $0 = g(x, \bar{z})$, we obtain the slow manifold as:

$$\bar{z} = H(x) = -\frac{\delta}{\lambda_f} x = -\beta x \tag{52}$$

The dynamics of the slow variable x is given by

$$\dot{x} = \left(\lambda_s - \frac{\mu\delta}{\lambda_f} \right) x + \mu y = \left(1 - \beta^2\right) \lambda_s x + \mu y \tag{53}$$

The numerical solution for the slow variable x at t_{n+1} is determined as

$$x_{n+1} = \hat{x} + \mu \int_{t_n}^{t_{n+1}} y(\tau) d\tau \tag{54}$$

where

$$\hat{x} = R\left((1 - \beta^2)\xi \right) x_n$$
$$R(s) = 1 + s + \frac{s^2}{2} + \frac{s^3}{6} + \frac{s^4}{24}$$

Eqn. (54) reduces to the following expression:

$$x_{n+1} = M_{11}x_n + M_{12}z_n \tag{55}$$

where

$$M_{11} = R\left((1-\beta^2)\xi\right) + \frac{\beta^2}{\alpha}(e^{\alpha\xi} - 1) - \frac{\beta^2}{\alpha^2}(\alpha\xi - e^{\alpha\xi} + 1)$$
$$M_{12} = \beta(e^{\alpha\xi} - 1) - \frac{\beta^3}{\alpha^2}(\alpha\xi - e^{\alpha\xi} + 1)$$

The numerical solution of z is determined as:

$$z_{n+1} = H(x_{n+1}) + y_{n+1} = M_{21}x_n + M_{22}z_n \tag{56}$$

where

$$M_{21} = -\beta M_{11} + \beta e^{(\alpha+\beta^2)\xi} + \frac{\beta(\beta^2-1)(M_{11} - e^{(\alpha+\beta^2)\xi})}{\alpha+\beta^2} - \frac{\beta(\beta^2-1)(e^{(\alpha+\beta^2)\xi} - 1)(M_{11}-1)}{(\alpha+\beta^2)^2\xi}$$
$$M_{22} = -\beta M_{12} + e^{(\alpha+\beta^2)\xi} + \frac{M_{12}\beta(\beta^2-1)}{\alpha+\beta^2} - \frac{M_{12}\beta(\beta^2-1)(e^{(\alpha+\beta^2)\xi} - 1)}{(\alpha+\beta^2)^2\xi}$$

The relationship between the two successive numerical solutions can be written in a matrix form as:

$$\begin{Bmatrix} x_{n+1} \\ z_{n+1} \end{Bmatrix} = \begin{bmatrix} M_{11} & M_{12} \\ M_{21} & M_{22} \end{bmatrix} \begin{Bmatrix} x_n \\ z_n \end{Bmatrix} = \mathbf{M} \begin{Bmatrix} x_n \\ z_n \end{Bmatrix} \tag{57}$$

where

$$M_{11} = R\left((1-\beta^2)\xi\right) + \frac{\beta^2}{\alpha}(e^{\alpha\xi} - 1) - \frac{\beta^2}{\alpha^2}(\alpha\xi - e^{\alpha\xi} + 1)$$
$$M_{12} = \beta(e^{\alpha\xi} - 1) - \frac{\beta^3}{\alpha^2}(\alpha\xi - e^{\alpha\xi} + 1)$$
$$M_{21} = -\beta M_{11} + \beta e^{\alpha\xi} + \frac{\beta}{\alpha}(e^{\alpha\xi} - 1)$$
$$M_{22} = -\beta M_{12} + e^{\alpha\xi} + \frac{\beta^2}{\alpha}(e^{\alpha\xi} - 1)$$

The proposed scheme is absolute stable if and only if the spectral radius of $\mathbf{M}$ is less than or equal to 1; i.e.,

$$\rho(\mathbf{M}) \leq 1 \tag{58}$$

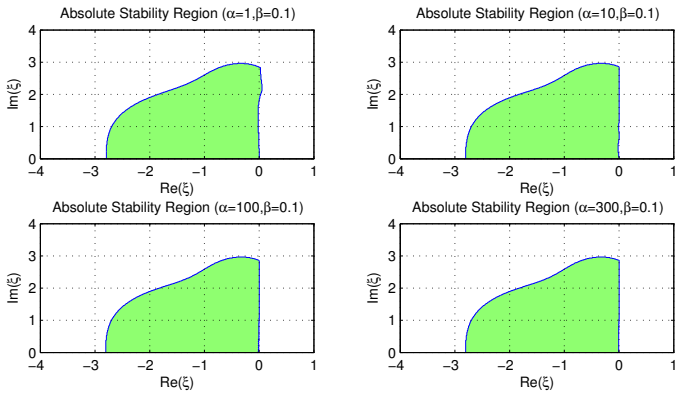

FIGURE 2. THE REGION OF ABSOLUTE STABILITY OF THE PROPOSE METHOD FOR DIFFERENT VALUES OF α

The region of absolute stability is the set of $\xi = h\lambda_s$ which satisfies the condition $\rho(\mathbf{M}) \leq 1$. Figures 2 and 3 show half of the region of absolute stability for different values of the parameters α and β. When β is zero, the state x and z are completely decoupled. The state z is solved by the analytic solution form of the linear system and the numerical solution is absolutely stable if

$$Re(h\lambda_f) \leq 0 \tag{59}$$

Therefore, the region of absolute stability is the intersection of the region of absolute stability of RK4 and the left half plane. As the parameter β increases, the region of the absolute stability changes slightly. So, the coupling between x and z does not have significant effect on the region of absolute stability. From Fig. 2, it can be seen that the region of absolute stability does not change much as the parameter α increases. It means that the region of absolute stability only depends on the eigenvalues of the slow variable and it is almost independent of the eigenvalues of the fast variable. As a result, the restriction on the step size h is weakened and the computational efficiency can be improved by employing a larger step size than the conventional numerical methods when multiple-timescale problems are solved.

ACCURACY ANALYSIS

In this section, we study the local error of the proposed method by using the linear test equation of Eqn. (50). The exact solutions for Eqn. (50) are denoted by $\hat{x}(t)$ and $\hat{z}(t)$ and they are given as

$$\begin{Bmatrix} \hat{x}(t) \\ \hat{z}(t) \end{Bmatrix} = e^{At} \begin{Bmatrix} x(0) \\ z(0) \end{Bmatrix} \tag{60}$$

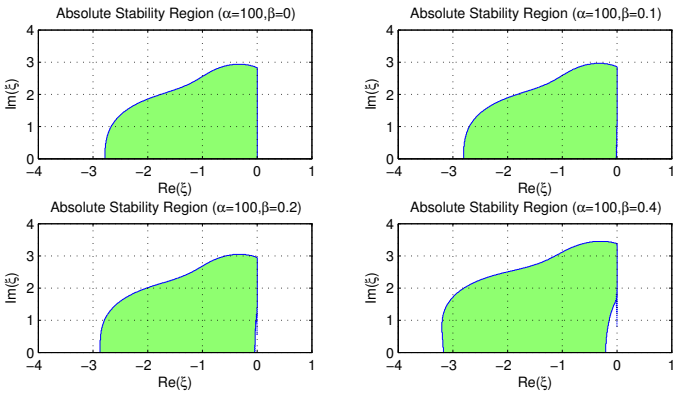

FIGURE 3. THE REGION OF ABSOLUTE STABILITY OF THE PROPOSE METHOD FOR DIFFERENT VALUES OF β

where

$$A = \begin{bmatrix} \lambda_s & \mu \\ \delta & \lambda_f \end{bmatrix}$$

The local errors of the state x and the state z are defined as

$$l_x(h) = |x(h) - \hat{x}(h)| \tag{61a}$$
$$l_z(h) = |z(h) - \hat{z}(h)| \tag{61b}$$

We choose λ_s and the initial condition as

$$\lambda_s = -1 + i,\ x(0) = 1,\ z(0) = 1 \tag{62}$$

Then, the local error is numerically computed and plotted with respect to stepsize h in Figs. 4 and 5. The slope of the graph, which is in log scale, represents the order of accuracy of the numerical method. The results show that the order of accuracy of the proposed method is one and the local error does not depend on the parameter α. The order of accuracy of RK4 is four but its local error is highly dependent on the parameter α. The accuracy of RK4 becomes worse as the parameter α increases. The results suggest that the proposed method will be useful when the system has states of two separate time scales and the coupling between them is weak.

It should be noted that the results do not account for the error which will be introduced by local linearization of $\dot{z} = g(x,z)$ since the test equation is linear. In this study, the order of accuracy of the proposed method is estimated numerically. More rigorous analysis of the accuracy will be attempted in the future.

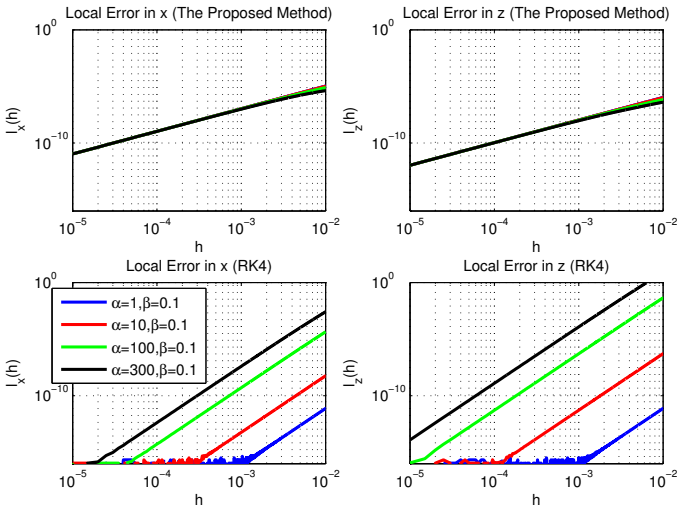

FIGURE 4. LOCAL ERROR VERSUS STEPSIZE FOR DIFFERENT VALUES OF α

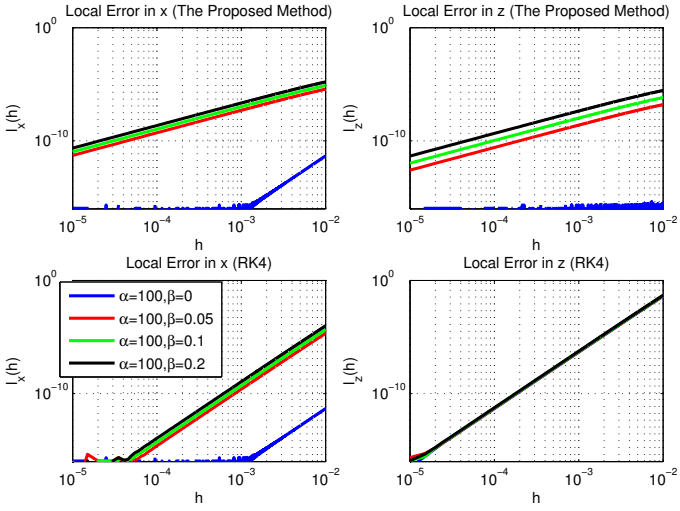

FIGURE 5. LOCAL ERROR VERSUS STEPSIZE FOR DIFFERENT VALUES OF β

NUMERICAL EXPERIMENTS

In this section, we consider a system containing a pendulum and a particle which has multiple-timescale characteristics in order to illustrate how the proposed numerical scheme integrates the differential equations of motion. The results will demonstrate that the proposed method can solve the equations of motion more efficiently compared to the Runge-Kutta method. This is due to relaxing the requirement for the absolute stability and using a larger step size when the proposed method is employed.

Figure 6 shows the configuration of the pendulum system. The meaning of the state variables and the physical parameters

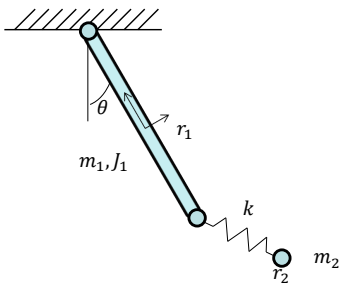

FIGURE 6. CONFIGURATION OF PENDULUM SYSTEM

and their values are:

$\mathbf{r}_1$: position of mass center of the bar
θ : rotation angle of the bar
m_1, J_1 : mass and inertia of the bar $(m_1 = 100, J_1 = 100)$
L : length of the bar $(L = 1)$
$\mathbf{r}_2$: position of the particle
m_2 : mass of the particle $(m_2 = 1e-5)$
k : spring coefficient $(k = 5)$

The equations of motion of the system are given as

$$\begin{bmatrix} m_1\mathbf{I} & 0 \\ 0 & J_1 \end{bmatrix} \begin{Bmatrix} \ddot{\mathbf{r}}_1 \\ \ddot{\theta}_1 \end{Bmatrix} = D^\top \lambda + \begin{Bmatrix} \mathbf{f}_1 \\ n_1 \end{Bmatrix} \tag{63a}$$

$$m_2 \ddot{\mathbf{r}}_2 = \mathbf{f}_2 \tag{63b}$$

where

$$\mathbf{g} = \begin{Bmatrix} 0 \\ -9.81 \end{Bmatrix}$$
$$\mathbf{f}_1 = m_1\mathbf{g} + \mathbf{f}_s$$
$$\mathbf{f}_2 = m_2\mathbf{g} - \mathbf{f}_s$$
$$n_1 = \mathbf{s} \times \mathbf{f}_s$$
$$\mathbf{f}_s = k\left(\mathbf{r}_2 - (\mathbf{r}_1 + \mathbf{s})\right)$$
$$\mathbf{s} = \begin{Bmatrix} L/2\sin\theta \\ -L/2\cos\theta \end{Bmatrix}$$
$$D = \begin{bmatrix} 1 & 0 & -L/2\cos\theta \\ 0 & 1 & -L/2\sin\theta \end{bmatrix}$$

The equations of motion for the pendulum is derived using the body-coordinate formulation [23] and the constraint equation for the revolute joint is given as

$$\Phi = \mathbf{r}_1 - \mathbf{s} = 0 \tag{64}$$

The position of the particle must exhibit high frequency dynamics due to the small value of m_2, which corresponds to the parameter ε in the standard singular perturbation model. Based on this observation, the state of the system is partitioned into the slow state x and the fast state z as

$$x = \begin{Bmatrix} \mathbf{r}_1 \\ \theta \\ \dot{\mathbf{r}}_1 \\ \dot{\theta} \end{Bmatrix}, \quad z = \begin{Bmatrix} \mathbf{r}_2 \\ \dot{\mathbf{r}}_2 \end{Bmatrix} \tag{65}$$

Then, the differential equation for z can be written as

$$\dot{z} = g(x,z) = \begin{Bmatrix} \dot{\mathbf{r}}_2 \\ -\frac{k}{m_2}\left(\mathbf{r}_2 - (\mathbf{r}_1 + \mathbf{s})\right) - \mathbf{g} \end{Bmatrix} \tag{66}$$

The slow manifold of the system is obtained by imposing $0 = g(x,\bar{z})$, which gives

$$\mathbf{r}_2 = \mathbf{r}_1 + \mathbf{s} - \frac{m_2}{k}\mathbf{g} \approx \mathbf{r}_1 + \mathbf{s} \tag{67}$$

The slow manifold corresponds to the quasi-steady-state case that the particle is rigidly attached to the end of the pendulum. This accounts for the limiting case that m_2 goes to zero. The boundary-layer system $y = z - \bar{z}$ represents the displacement of the particle relative to the end point of the pendulum.

This system of differential equation is solved by using the proposed method, RK4 and ode45 [24]. For the proposed method and RK4, the step size is chosen to be $h = 0.005$. Figure 7 compares the numerical solutions from those numerical methods. It can be seen that RK4 yields an unstable solution, since the step size h does not satisfy the absolute stability condition. The eigenvalue of the fast variable is approximately $\lambda_f \approx (k/m_2)i = 5 \times 10^5 i$. With the choice of $h = 0.005$, $\xi = h\lambda_f \approx 2.5 \times 10^3 i$ is located outside the region of absolute stability of RK4 that has been shown in Fig. 1.

The proposed method gives a stable solution with the step size $h = 0.005$. This is possible since the region of absolute stability of the proposed method only depends on the eigenvalues of the slow variable x. The proposed method can maintain the absolute stability with a larger step size and it leads to better computational efficiency. Figure 7 shows that the computation time of the proposed method is about 60% of that of ode45.

The total energy of the system should be constant because the system has no damping. The total energy of the system can be computed as

$$\begin{aligned} E = &\frac{1}{2}m_1|\dot{\mathbf{r}}_1|^2 + \frac{1}{2}J_1\dot{\theta}^2 + \frac{1}{2}m_2|\dot{\mathbf{r}}_2|^2 \\ &+ 9.81\left(m_1 r_{1y} + m_2 r_{2y}\right) + \frac{1}{2}k|\mathbf{r}_2 - (\mathbf{r}_1 + \mathbf{s})|^2 \end{aligned} \tag{68}$$

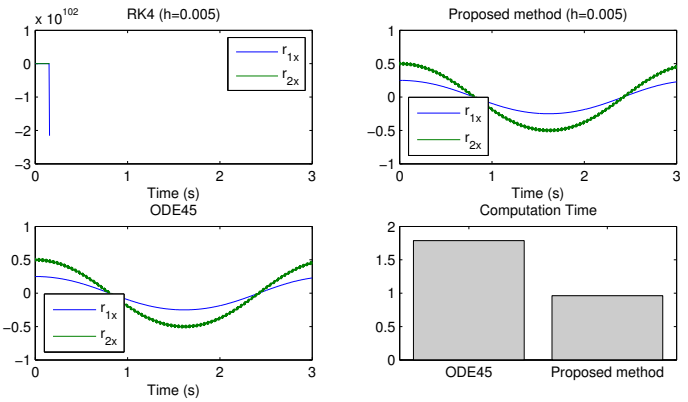

FIGURE 7. COMPARISON OF SIMULATION RESULTS FOR PENDULUM

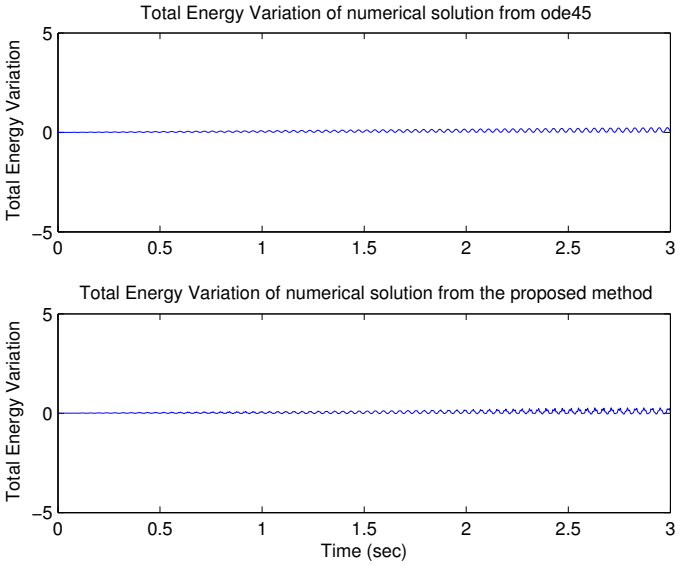

FIGURE 8. TOTAL ENERGY VARIATION OF NUMERICAL SOLUTIONS

Figure 8 compares the total energy variation of the numerical solutions obtained by ode45 and the proposed method. It can be seen that the proposed method provides comparable accuracy with larger step size than a conventional method like ode45.

CONCLUSION

In this study, a numerical integration method is introduced which utilizes the local linearization method and the singular perturbation theory to deal with the coupling between the fast and slow variables. This method can capture the transient dynamics by the successive linear approximation, and the dynamics of the slow variable is computed by a conventional numerical method with the help of the invariant manifold. The absolute stability condition and accuracy of the proposed method was analyzed and its advantage was demonstrated by numerical experiments. The numerical experiments showed that the proposed method can solve multiple-timescale problems with better numerical efficiency. This is due to relaxing the requirement of the step size for the absolute stability and allowing larger time steps.

ACKNOWLEDGMENT

G. Gil would like to acknowledge the financial support of Hankook Tire in this research project.

REFERENCES

[1] Khalil, H., 2002. *Nonlinear systems*. Prentice Hall, Upper Saddle River, N.J.

[2] Günther, M., and Rentrop, P., 1993. "Multirate row methods and latency of electric circuits". *Appl. Numer. Math.,* ***13***, pp. 83–102.

[3] Kopf, A., Paul, W., and Dunweg, B., 1997. "Multiple time step integrators and momentum conservation". *Computer Physics Communications,* ***101***, pp. 1–8.

[4] Tuckerman, M., and Berne, B., 1991. "Molecular dynamics in systems with multiple time scales: Systems with stiff and soft degrees of freedom and with short and long range forces". *J. Chem. Phys.,* ***95***(11), pp. 8362–8364.

[5] Engstler, C., and Lubich, C., 1997. "Multirate extrapolation methods for differential equations with different time scales". *Computing,* ***58***, pp. 173–185.

[6] Shome, S., Haug, E., and Jay, L., 2004. "Dual-rate integration using partitioned runge-kutta methods for mechanical systems with interacing subsystems". *Mechanics Based Design of Structures and Machines,* ***32***(3), pp. 253–282.

[7] Solcia, T., and Masarati, P., 2011. "Multirate simulation of complex multibody systems". In Multibody Dynamics 2011, ECCOMAS Thematic Conference.

[8] Arnold, M., 2007. "Multi-rate time integration for large scale multibody system models". In *IUTAM Symposium on Multiscale Problems in Multibody System Contacts*, P. Eberhard, ed., Vol. 1 of *IUTAM Bookseries*. Springer Netherlands, pp. 1–10.

[9] Jimenez, J., Biscay, R., Mora, C., and Rodriguez, L., 2002. "Dynamic properties of the local linearization method for initial-value problems". *Applied Mathematics and Computation,* ***126***, pp. 63–81.

[10] Jimenez, J., and Carnodell, F., 2005. "Rate of convergence of local linearization schemes for initial-value problems". *Applied Mathematics and Computation,* ***171***, pp. 1282–1295.

[11] Kokotovic, P., Khalil, H., and O'Reilly, J., 1999.

Singular perturbation methods in control : analysis and design. Society for Industrial and Applied Mathematics, Philadelphia.

[12] Ghorbel, F., and Spong, M. W., 2000. "Integral manifolds of singularly perturbed systems with application to rigid-link flexible-joint multibody systems". *International Journal of Non-Linear Mechanics,* ***35***(1).

[13] Khalil, H., 1987. "Stability analysis of nonlinear multiparameter singularly perturbed systems". *IEEE Transactions on Automatic Control,* ***32***(3).

[14] Sanfelice, R. G., and Teel, A. R., 2011. "On singular perturbations due to fast actuators in hybrid control systems". *Automatica,* ***47***(4).

[15] Lam, S. H., 1993. "Using CSP to understand complex chemical kinetics". *Combustion Science and Technology,* ***89***.

[16] Lam, S. H., and Goussis, D. A., 1994. "The CSP method for simplifying kinetics". *International Journal of Chemical Kinetics,* ***26***(4).

[17] Zagaris, A., Kaper, H. G., and Kaper, T. J., 2004. "Fast and slow dynamics for the computational singular perturbation method". *Multiscale Modeling and Simulation,* ***2***(4).

[18] Aiken, R. C., and Lapidus, L., 1974. "An effective numerical integration method for typical stiff systems". *Aiche Journal,* ***20***(2).

[19] Miranker, W., 1973. "Numerical methods of boundary layer type for stiff systems of differential equations". *Computing,* ***11***(3).

[20] Miranker, W., 1981. *Numerical methods for stiff equations and singular perturbation problems*. D. Reidel distributed in the U.S.A. and Canada by Kluwer Boston, Dordrecht, Holland Hingham, MA.

[21] Loan, C. F. V., 1978. "Computing integrals involving the matrix exponential". *IEEE Transactions on Automatic Control,* ***23***(3).

[22] Ascher, U., and Petzold, L., 1998. *Computer methods for ordinary differential equations and differential-algebraic equations*. Society for Industrial and Applied Mathematics, Philadelphia.

[23] Nikravesh, P., 2008. *Planar multibody dynamics : formulation, programming, and applications*. CRC Press, Boca Raton.

[24] MATLAB, 2011. *version 7.13.0 (R2011b)*. The MathWorks Inc., Natick, Massachusetts.